EUROPHYSICS LETTERS 1 August 2004

Europhys. Lett., **67** (3), pp. 418–424 (2004)
DOI: 10.1209/epl/i2004-10076-x

Twist-bend instability for toroidal DNA condensates

I. M. Kulić, D. Andrienko and M. Deserno
Max-Planck-Institut für Polymerforschung - Ackermannweg 10, 55128 Mainz, Germany

(received 17 March 2004; accepted in final form 19 May 2004)

PACS. 64.70.Nd – Structural transitions in nanoscale materials.
PACS. 87.15.He – Dynamics and conformational changes.
PACS. 61.30.Pq – Microconfined liquid crystals: droplets, cylinders, randomly confined liquid crystals, polymer dispersed liquid crystals, and porous systems.

Abstract. – We propose that semiflexible polymers in poor solvent collapse in two stages. The first stage is the well-known formation of a dense toroidal aggregate. However, if the solvent is sufficiently poor, the condensate will undergo a second structural transition to a twisted entangled state, in which individual filaments lower their bending energy by additionally orbiting around the mean path along which they wind. This "topological ripening" is consistent with known simulations and experimental results. It connects and rationalizes various experimental observations ranging from strong DNA entanglement in viral capsids to the unusually short pitch of the cholesteric phase of DNA in sperm heads. We propose that topological ripening of DNA toroids could improve the efficiency and stability of gene delivery.

Introduction. – Single polymers collapse from a random coil conformation to a dense state once the solvent gets sufficiently poor [1]. For a flexible chain the condition of minimal surface energy yields an approximately spherical globule, but for semiflexible polymers the situation is more complex [2]: The local structure of the dense phase then consists of essentially straight chains with a basically parallel alignment, in order to minimize bending energy and maximize density, respectively. Such a state can be characterized by a smooth field of tangent vectors, but in the spherical case this field must have at least two energetically unfavorable defects on the surface (one cannot comb a sphere). However, for a *torus* many defect-free fields are possible. Indeed, DNA, the probably best studied semiflexible polymer, readily forms beautiful nanotori after adding any one of a variety of possible condensing agents (like polyethylenglycol (PEG), multivalent counterions, or bundling proteins) to a dilute solution of DNA chains [3]. These tori are surprisingly monodisperse, having a radius comparable to the persistence length of DNA ($\ell_\mathrm{p} \approx 50\,\mathrm{nm}$) basically independent of the condensation method [3].

Consider such a condensate, in which the chain is wound up like a garden hose to form a torus with axial and tubular radii r_1 and r_2, respectively. Since r_1 is the average radius of curvature of the chain, a simple scaling analysis balancing a bending energy A/r_1^2 per unit length of polymer, where $A = k_\mathrm{B}T\ell_\mathrm{p}$ is the bending modulus of a semiflexible chain, and a surface energy σ per unit area of the torus yield [2] $r_1 \sim (\sigma/A)^{-2/5}V^{1/5}$ and $r_2 \sim (\sigma/A)^{1/5}V^{2/5}$, where the chain volume $V \sim r_1 r_2^2$ as well as the packing density are assumed constant. Hence, the *slenderness* $\xi = r_1/r_2 \sim (\sigma/A)^{-3/5}V^{-1/5}$ shrinks if σ or V increase (*i.e.*, if the solvent gets poorer or the chain longer), and thus the torus "fattens". In this

case it is no longer justified to calculate the bending energy with some average radius of curvature $\langle\rho\rangle = r_1$. In fact, since $\langle\rho^{-2}\rangle \geq \langle\rho\rangle^{-2}$ (by virtue of Jensen's inequality [4]), the actual curvature energy should be larger. However, the same argument indicates that the condensate can *lower* its bending energy by redistributing curvature more evenly. In this letter we demonstrate that indeed below a critical slenderness ξ_c (or above a critical surface tension σ_c) the system spontaneously relaxes bending energy by *twisting* the bundle of polymer strands. In other words, given that the overall *shape* of the condensate is a torus, its internal *structure* still depends on further elastic details. However, the underlying mechanism is very generic and thus independent of specific microscopic details of the polymer under study.

Indirect indications of such a twisted state can be found in computer simulations [5]. Analyzing Cryo-EM experiments on DNA toroids [6] Hud *et al.* proposed a rosette-like DNA winding (slowly precessing off-centered loops which yield a "spirograph" motif) [7]. Furthermore, such a non-trivial *local* organization of DNA in toroids suggests natural explanations for various remarkable *large-scale* findings from *in vivo* studies: Certain bacteriophages, whose DNA is (due to a genetic modification) no longer end-attached to their nucleocapsid, display unusually strong knotting of the genome [8]. DNA toroids released from giant T4 phages can undergo supercoiling [9]. And the chirality of the highly confined sperm-chromatin is surprisingly pronounced, with a pitch 10 times shorter than *in vitro* [10]. These facts make us wonder whether there is a connection to the topological ripening we will now discuss.

Nematic elastic-energy functional. – Let us begin our quantitative analysis of the situation by neglecting the connectivity of the chain. More specifically, we will first formulate a *local* theory which is based on the above-mentioned nematic field $\boldsymbol{n}$ of unit tangent vectors [11]. The path of the actual polymer will later be recovered as an integral curve of this flow field, and its global topological properties can then be studied. The elastic energy e per unit volume, describing the deviation from perfectly parallel alignment, is the Frank-Oseen free energy density of a uniaxial nematic liquid crystal [12]:

$$e = \frac{1}{2}K_1[\nabla\cdot\boldsymbol{n}]^2 + \frac{1}{2}K_2[\boldsymbol{n}\cdot(\nabla\times\boldsymbol{n})]^2 + \frac{1}{2}K_3[\boldsymbol{n}\times(\nabla\times\boldsymbol{n})]^2, \tag{1}$$

where the three terms correspond to splay, twist, and bend deformations, respectively [13]. Assuming the condensate to behave like an incompressible liquid (thereby accounting for excluded-volume effects in an effective way), the first term (splay) must vanish identically in order to maintain a constant polymer density throughout the condensate [14], while the other two terms divide the elastic energy between themselves. The total energy is of course the integral of eq. (1) over the torus volume.

It is convenient to treat this situation in suitable toroidal coordinates $\{r, \vartheta, \varphi\}$, defined by

$$x = (r_1 - r\cos\vartheta)\cos\varphi, \qquad y = (r_1 - r\cos\vartheta)\sin\varphi, \qquad z = r\sin\vartheta. \tag{2}$$

The nematic field is now represented as $\boldsymbol{n} = n_r\boldsymbol{e}_r + n_\vartheta\boldsymbol{e}_\vartheta + n_\varphi\boldsymbol{e}_\varphi$ (where the $\boldsymbol{e}_i = \partial_i\boldsymbol{r}/|\partial_i\boldsymbol{r}|$ are the toroidal unit tangent vectors). When inserting this into eq. (1) and integrating over the volume, we obtain the elastic energy as a functional of $n_r(r,\vartheta,\varphi)$, $n_\vartheta(r,\vartheta,\varphi)$, and $n_\varphi(r,\vartheta,\varphi)$. At the surface of the torus the boundary condition $n_r(r = r_2) = 0$ must hold, and owing to rotational symmetry we will henceforth make the (nontrivial but very reasonable) assumption that none of the coordinate functions depends on φ. These steps reduce the task of finding the optimal polymer winding to a two-dimensional variational problem.

Numerical minimization. – Now that the mathematical problem is formulated, let us first have a look at the full solution, which we obtained numerically via a conjugate gradient minimization [15]. The results confirm the suspicions made above: For large enough slenderness

Fig. 1

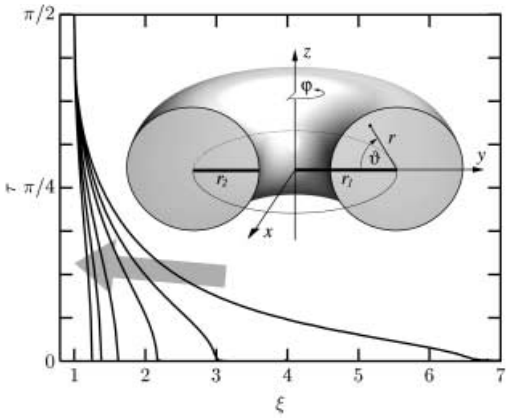

Fig. 2

Fig. 1 – Illustration of the flow field on a toroidal condensate which features additional twist. The slenderness of the torus is $\xi = 1.5$.

Fig. 2 – Twist order parameter $\tau \equiv \arccos(n_{\varphi,\min})$ as a function of the slenderness $\xi = r_1/r_2$. The curves correspond to different ratios of elastic moduli, $\eta = K_2/K_3 \in \{0.01, 0.05, 0.1, 0.2, 0.3, 0.4\}$, the gray arrow pointing toward increasing values. The inset illustrates the toroidal coordinate system.

$\xi = r_1/r_2$, the equilibrium nematic field is $\boldsymbol{n} = \boldsymbol{e}_\varphi$, corresponding to simple circumferential winding of the polymer. But as the torus grows sufficiently fat, a continuous transition occurs to a state in which (simultaneously throughout the entire torus) $\boldsymbol{n}$ acquires components in $\boldsymbol{e}_\vartheta$- and $\boldsymbol{e}_r$-direction, *i.e.*, the polymer additionally winds around the tubular circle, see fig. 1. This winding relaxes bending energy, but only at the expense of the additional twist, which is zero when $\boldsymbol{n} = \boldsymbol{e}_\varphi$. Consequently, this twist instability occurs more readily if the ratio $\eta = K_2/K_3$ of twist and bend modulus is small. All this is confirmed in fig. 2, where we show the maximum twist angle $\tau \equiv \arccos(n_{\varphi,\min})$, which is a suitable order parameter, as a function of the slenderness ξ of the torus. Note that the calculation is reliable down to the value $\xi = 1$, where the hole in the torus degenerates to a point; here the only possible tangent vector is $\boldsymbol{e}_\vartheta$ and thus $\tau = \pi/2$.

Variational ansatz. – The mathematical task of functional minimization can often be accurately approximated by devising a variational ansatz which is analytically tractable. The following choice turns out to be remarkably good: We will first assume that the nematic field does not have a component in $\boldsymbol{e}_r$-direction. The tangential boundary condition $n_r(r = r_2) = 0$ is then automatically taken care of. The remaining two components must satisfy the normalization condition $n_\vartheta^2 + n_\varphi^2 = 1$, and it thus suffices to specify one of them, say n_ϑ. It is easy to check that any ansatz of the form $n_\vartheta = f(r)/[1 - (r/r_1)\cos\vartheta]$ with an arbitrary function $f(r)$ yields a divergence-free nematic field. We choose a linear $f(r) = \omega r/r_2$, *i.e.*

$$n_\vartheta(r, \vartheta; \omega) = \omega \, \frac{r/r_2}{1 - (r/r_1)\cos\vartheta} \,, \tag{3}$$

where ω, which we may call the "twisting strength", is the only free parameter of the ansatz. With this choice we go back into the Frank-Oseen free energy (1), calculate the derivatives, and integrate over the volume of the torus. Since the sign of ω only determines the *handedness* of the twisted structure, it cannot influence the free energy E, which thus must be an even

function of ω [13]. An expansion in powers of ω^2 then yields

$$\frac{E}{K_3\, r_2} = g_0(\xi) + g_2(\xi,\eta)\,\omega^2 + g_4(\xi,\eta)\,\omega^4 + \mathcal{O}\big(\omega^6\big), \tag{4}$$

where the expansion coefficients g_i are functions of the system parameters [16]. In particular,

$$g_0(\xi) = 2\pi^2\big(\xi - \sqrt{\xi^2-1}\big) \stackrel{\xi\to\infty}{\longrightarrow} \pi^2/\xi\,. \tag{5}$$

This term contributes even if the twist ω vanishes. In fact, it coincides with the bending energy of a chain of length L which has a curvature energy A/ρ^2 per unit length (ρ being the local radius of curvature), and which is wound without additional looping within a torus of volume V —provided the (intuitively clear) relation $K_3V = AL$ holds. This relates the nematic bending modulus K_3 to the more usual polymer bending stiffness A.

While g_0 helped us to map our parameters, g_2 will localize the phase transition. The reason is that eq. (4) has the form of a Landau free energy as it occurs for phase transitions with a scalar order parameter, ω, and it predicts a continuous transition (which breaks chiral symmetry) at the point where the coefficient of the quadratic term vanishes, *i.e.*, $g_2(\xi,\eta) = 0$. This results in the phase boundary

$$\eta = \frac{1}{2} + \frac{\xi^2-1}{4\,\xi^2}\big[1 + 6\,\xi\big(\sqrt{\xi^2-1} - \xi\big)\big]. \tag{6}$$

This boundary is shown in fig. 3, together with exact points originating from the full functional minimization. It quantifies the conclusion that toroidal condensates will spontaneously twist if the slenderness $\xi = r_1/r_2$ is small (and the torus thus fat), and if the ratio of elastic moduli $\eta = K_2/K_3$ is small, *i.e.* if twisting a bundle is easy compared to bending it. For large ξ, eq. (6) asymptotically behaves like $\eta \sim \frac{5}{16}\xi^{-2}$, thereby explaining the exponent -2, which is also indicated in fig. 3 and which actually describes the whole phase boundary quite well. The agreement between the simple one-parameter variational ansatz and the full calculation is remarkably good. It can even be improved by including an additional prefactor $1 - \frac{r}{r_1}$ into eq. (3). Particularly for small ξ this improved ansatz agrees better with the exact answer, basically since the new prefactor cancels the unphysical divergence of the denominator for $r \to r_1$ at $\vartheta = 0$. The analytical expression for the phase boundary is quite involved and will not be shown here, but it has the same large ξ asymptotics (see fig. 3).

Both the ansatz as well as the full numerical solution point to an upper critical ratio of elastic moduli, η_c, beyond which the system will no longer spontaneously twist. Even at the lowest possible slenderness $\xi = 1$, the energetic cost for twisting has become so large that it no longer admits a bending relaxation. The ansatz (3) gives $\eta_c = \frac{1}{2}$, the improved ansatz gives $\eta_c \approx 0.829$, while the full numerical solution suggests the deceptively simple result $\eta_c = 1$. We have no analytical support for the latter, but we also note that the limit $\xi \to 1$ is somewhat academic, because our tacit assumption that the condensate shape is strictly toroidal will most likely break down in this case [17].

We have thus seen that the elastic constant ratio η and the torus slenderness ξ uniquely specify the twist-state of the condensate. However, while one can easily measure ξ in an experiment (just by visual inspection), it is hard to specify in advance. In contrast to that, the surface tension σ can be readily changed (for instance via the concentration of condensing agents), but its actual value is hard to measure. In our simple model it is of course not difficult to add a tension term σ times the torus surface S to the condensate energy. Using $S \propto \xi^{1/3}V^{2/3}$, one can re-express the twisting transition as being driven by increasing σ,

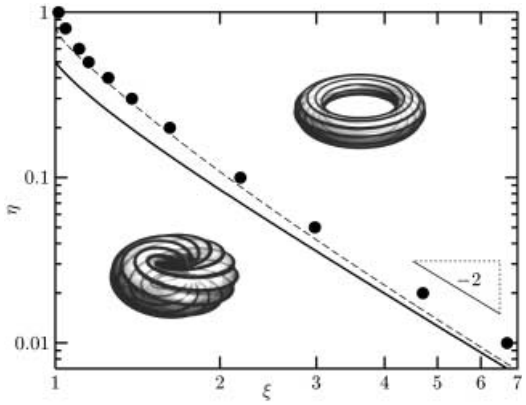

Fig. 3

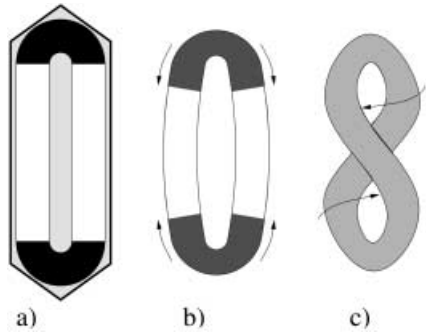

Fig. 4

Fig. 3 – Structural phase diagram of the toroidally wound complex on a log-log scale. For small $\xi = r_1/r_2$ and $\eta = K_2/K_3$, the polymer is wound in a twisted way, for large ξ and η it prefers to wind straight. The dots are results from the full numerical minimization, the solid line is eq. (6), and the dashed line stems from the "improved ansatz" (see the text).

Fig. 4 – Possible mechanism for plectonemic supercoiling [9] of the genome of giant T4 phages: (a) Initially the toroidal genome is only twisted (dark shading) at the two poles. (b) After removing the capsid, twist propagates into the remaining DNA, but since the twist-creating confinement is removed, the remaining bundle suddenly is overtwisted. (c) This then induces a global supercoiling.

and it remains continuous. However, practical considerations suggest that one tunes σ only for the purpose of modifying ξ, but subsequently use ξ as the independent variable. This way one needs no longer (neither theoretically nor practically) worry about how a particular concentration of condensing agents gives rise to a particular torus geometry.

Global aspects. – After these local considerations, it is time to study global aspects of the polymer structure, *i.e.*, consequences of the chain *connectivity* which we have neglected so far. Let us start with the flow itself. It can be shown that incompressibility, $\nabla \cdot \boldsymbol{n} = 0$, together with axial symmetry causes the flow to be Hamiltonian —hence one more conservation law exists [18]. In our case, it forces the flow lines to stay on two-dimensional slightly deformed toroidal surfaces, such that the total flow consists of a nested structure of invariant tori. In fact, our ansatz (3) follows readily from the quadratic Hamiltonian $H = \frac{1}{2}\xi\omega r^2$, which is constant on circular tubular layers. Of course, the actual polymer has to switch between these layers, reminding us that, irrespective of twist, none of the above structures can be realized without localized defects [19], even if the underlying nematic flow field is everywhere smooth.

There is one global aspect of the polymer structure in which it differs fundamentally from a plainly wound torus: As is visible in fig. 1, the path of the polymer threads it repeatedly through the middle hole. Moreover, the amount of this looping (as measured, *e.g.*, by the average change in ϑ per turn) depends on the layer. This effect implies that the entire polymeric strand is heavily entangled with itself. A rough estimate for $\xi = 1.5$ and polymer length $L = 15\,\mu$m gives about 30 threadings through the hole. In fact, were it not for the two free ends, these knotted states would be topologically inaccessible. In other words, unlike the initial collapse, the second stage, the structural ripening, relies on the motion of the free chain ends and is thus a much slower process.

On the other hand, this structural ripening meets no kinetic barriers during the relaxation to its twisted ground state, as it proceeds downhill on the free-energy landscape. The motion of the two free ends is then energetically directed and their local rearrangement does not involve the highly improbable threading through the toroid hole in 3D space. In addition, the weak chiral interaction of DNA molecules [10] neglected above gives rise to a (small) chiral term in the elastic free energy, which might contribute to the symmetry breaking and "guide" the twisting in a preferred direction.

Discussion. – Is the predicted effect strong enough to be of some relevance for DNA condensation? For typical experimental parameters of DNA length $L = 15$–$30\,\mu$m, $\xi \sim 1.5$–2.5, bending stiffness $A \sim 50 k_{\mathrm{B}}T \cdot$nm, and inter-helical distance $d \sim 3$ nm we obtain first the elastic constant $K_3 \sim A/d^2 \sim 20$ pN, which is dominated by the bending stiffness [11]. The twist constant K_2 can be estimated by the decondensation force ~ 2 pN obtained in single-molecule experiments with condenser spermidine [20]. Then the difference in elastic energy between the twisted and untwisted states, as bounded below by the the variational ansatz, lies in the range 15–$30 k_{\mathrm{B}}T$. This indicates that topological ripening stabilizes the condensate. In addition, if the solvent quality abruptly improves, the twisted torus will unfold more inertly than its untwisted counterpart, due to heavy entanglement with itself. If this stabilization occurs on the typical time scales relevant for gene therapeutical applications, it might prevent a premature digestion of the genetic material by the host organism and influence (positively) the efficiency of the gene delivery process.

Finally, it is tempting to speculate that the twist-bend instability is responsible for several puzzling phenomena observed in biology. For instance, sperm chromatin shows an unusually short DNA cholesteric pitch (10 times shorter than *in vitro*) [10]. Since the genome is highly confined in sperm cells, basically at the same density as the DNA tori discussed above, it is potentially prone to a twist-bend instability (recall that all one really needs is an externally imposed bending of a bundle of DNA). While the weak intrinsic DNA chirality might thus determine the *handedness* of the resulting twist, its *pitch* would then be given by the twisted state of polymer strands after the topological ripening took place. As a second example, if the capsid of bacterial phages is broken (for instance, by osmotic shock), their DNA spills onto the underlying substrate. The amount of "knotting" displayed by the freed genome is significantly larger for genetically modified phages, in which the end of the viral genome is not first attached to the capsid at the time of loading it [8]. Since the ends are free to move, the torus- or spool-like genome inside such mutant phages can again undergo topological ripening, explaining the enhanced entanglement of DNA after breaking the capsid. Finally, Earnshaw *et al.* [9] have shown that when mutant T4 bacteriophages (displaying a greatly enhanced capsid aspect ratio) are opened under conditions in which the toroidally wound-up genome remains condensed, structures resembling "twisted skeins of yarn" are sometimes observed (see figs. 5 and 7 in ref. [9]). Within the framework of the twist-bend instability discussed in the present letter, the following explanation is tempting (see fig. 4): Inside the elongated phage head, the genome is present as a torus which is squeezed flat, and only at the two "poles" curvature exists which promotes the creation of twist. After opening the capsid, the torus can resume a properly round shape. Its rather slender shape no longer necessitates a twist, but for kinetic reasons it cannot instantaneously get rid of it. However, it can rather quickly exchange twist for *writhe* [21] and thus undergo *plectonemic supercoiling*, a state which indeed characterizes the observed structures rather accurately. Since supercoiling inherits its handedness from the underlying twist, which itself emerged via spontaneous breaking of chiral symmetry, both right- and left-handed supercoiled states should exist, which indeed appears to be borne out by observation [9].

* * *

We thank H. Schiessel, K. Kremer, I. Pasichnyk, and A. Ryskin for helpful discussions. MD acknowledges financial support from the German Science Foundation under grant De775/1-2.

REFERENCES

[1] Grosberg A. Y. and Khokhlov A. R., *Statistical Physics of Macromolecules* (AIP Press) 1994; Lifshitz I. M., Grosberg A. Y. and Khokhlov A. R., *Rev. Mod. Phys.*, **50** (1978) 683.
[2] Grosberg A. Y., *Biofizika*, **24** (1979) 32; Grosberg A. Yu. and Khokhlov A. R., *Adv. Polym. Sci.*, **41** (1981) 53.
[3] Bloomfield V. A., *Curr. Opin. Struct. Biol.*, **6** (1996) 334; *Biopolymers*, **44** (1997) 269.
[4] A convex function $f(x)$ lies above any of its tangents. Constructing the tangent at $x = \langle x\rangle$ shows that $f(x) \geq f(\langle x\rangle) + (x - \langle x\rangle)f'(\langle x\rangle)$. Averaging yields Jensen's inequality $\langle f(x)\rangle \geq f(\langle x\rangle)$. For concave f the inequality sign reverses. Jensen J. L. W. V., *Acta Math.*, **30** (1906) 175.
[5] Stevens M. J., *Biophysical J.*, **80** (2001) 130; Stukan M. R. *et al.*, *J. Chem. Phys.*, **118** (2003) 3392.
[6] Marx K. A. and Ruben G. C., *Nucl. Acids Res.*, **11** (1983) 1839.
[7] Hud N. V., Downing K. H. and Balhorn R., *Proc. Natl. Acad. Sci. USA*, **92** (1995) 3581.
[8] Liu L. F. *et al.*, *Proc. Natl. Acad. Sci. USA*, **78** (1981) 5498; Arsuaga J. *et al.*, *Proc. Natl. Acad. Sci. USA*, **99** (2002) 5373.
[9] Earnshaw W. C., King J., Harrison S. C. and Eiserling F. A., *Cell*, **14** (1978) 559.
[10] Livolant F., *Physica A*, **176** (1991) 117; Livolant F. and Leforestier A., *Prog. Polym. Sci.*, **21** (1996) 1115.
[11] de Gennes P. G., *Mol. Cryst. Liq. Cryst. Lett.*, **34** (1977) 177; Meyer R., in *Polymer Liquid Crystals*, edited by Cifferi A. *et al.* (Academic Press, New York) 1982; Strey H. H., Parsegian V. A. and Podgornik R., *Phys. Rev. E*, **59** (1999) 999.
[12] de Gennes P. G. and Prost J., *The Physics of Liquid Crystals*, 2nd edition (Clarendon Press, Oxford) 1995.
[13] Here we neglect the usually weak cholesteric interaction [10] stemming from DNA chirality.
[14] In infinitely long polymer liquid crystals without hairpins, the splay strongly couples to density variations [11].
[15] Press W. H., Flannery B. P., Teukolsky S. A. and Vetterling W. T., *Numerical Recipes in Fortran*, 2nd edition (Cambridge University Press, Cambridge) 1992.
[16] For the particular ansatz (3), the resulting coefficient g_4 does in fact not depend on η; but generally it does.
[17] Ubbink J. and Odijk T., *Europhys. Lett.*, **33** (1996) 353.
[18] The following transformation of the field and coordinates given in a cylindrical coordinate system, $\{\rho, z\} \to \{\rho^2/2, z\}$, $\{n_\rho, n_z\} \to \{\rho n_\rho, n_z\}$, together with the axial symmetry, reduces the 3D divergence-free nematic field to the (new) 2D divergence-free field. Then, the director field can be written as $n_\rho = \rho^{-1}\partial H/\partial z$, $n_z = -\rho^{-1}\partial H/\partial\rho$, where $H(\rho, z)$ is the Hamiltonian.
[19] For hexagonal-crystalline toroids this effect was pointed out by Park S. Y., Harries D. and Gelbart W. M., *Biophys. J.*, **75** (1998) 714.
[20] Baumann C. G. *et al.*, *Biophys. J.*, **78** (2000) 1965; Murayama Y., Sakamaki Y. and Sano M., *Phys. Rev. Lett.*, **90** (2003) 018102.
[21] Fuller F. B., *Proc. Natl. Acad. Sci. USA*, **68** (1971) 815; **75** (1978) 3557.